UCRL-JRNL-201883

LAWRENCE
LIVERMORE
NATIONAL
LABORATORY

Irradiation swelling behavior and its dependence on temperature, dose rate and dislocation structure evolution

M. P. Surh, J. B. Sturgeon, W. G. Wolfer

January 16, 2004

Journal of Nuclear Materials

Disclaimer

This document was prepared as an account of work sponsored by an agency of the United States Government. Neither the United States Government nor the University of California nor any of their employees, makes any warranty, express or implied, or assumes any legal liability or responsibility for the accuracy, completeness, or usefulness of any information, apparatus, product, or process disclosed, or represents that its use would not infringe privately owned rights. Reference herein to any specific commercial product, process, or service by trade name, trademark, manufacturer, or otherwise, does not necessarily constitute or imply its endorsement, recommendation, or favoring by the United States Government or the University of California. The views and opinions of authors expressed herein do not necessarily state or reflect those of the United States Government or the University of California, and shall not be used for advertising or product endorsement purposes.

This work was performed under the auspices of the U.S. Department of Energy by the University of California, Lawrence Livermore National Laboratory under Contract No. W-7405-Eng-48.

Irradiation swelling behavior and its dependence on temperature, dose rate, and dislocation structure evolution

Michael P. Surh, J. B. Sturgeon and W. G. Wolfer
Lawrence Livermore National Laboratory Livermore, California, 94550, USA

(Dated: January 13, 2004)

Abstract

The microstructural evolution of high purity steel under irradiation is modeled including a dislocation density that evolves simultaneously with void nucleation and growth. The predicted void swelling trends versus temperature, flux, and time are compared to experiment and to earlier calculations with a fixed dislocation density. The behavior is further analyzed within a simplified picture of segregation of irradiation defects to microstructural sinks. Agreement with experimental swelling behavior improves when dislocations co-evolve with the void content versus simulations with a fixed dislocation density. The time-dependent dislocation content dictates the rate of void nucleation and shapes the overall void size distribution so as to give steady swelling behavior over long times.

I. INTRODUCTION

Irradiation-induced swelling in reactor steels commonly exhibits an incubation period during which the volume change initially remains small despite the increasing irradiation dose [1]. The duration of this incubation stage commonly depends on temperature, dose rate, and initial characteristics like dislocation content and solute concentrations [1–7]. Eventually, the swelling rate accelerates to a value of 1%/dpa (displacement per atom) for stainless steel. Once achieved, this rate is fairly constant over many subsequent dpa of irradiation. It is also largely independent of temperature and flux over wide ranges. The swelling is driven by competition among dislocations, defect clusters, and stable voids for the mobile defects created by damage cascades. Stress-mediated interactions lead to a preferential segregation of interstitials (or mobile interstitial clusters) at climbing dislocations, and a corresponding net influx of vacancies at growing voids and vacancy clusters [8–10]. Swelling does not occur absent growing voids because dislocations then absorb equal numbers of vacancies and interstitials on average.

Recently, simulations of void evolution and irradiation swelling behavior have been analyzed for a model with a constant dislocation density [11]. This simplification allows study of void nucleation and growth in isolation from other, concurrent changes in the microstructure. The model successfully reproduces transient incubation-like behavior followed by quasi-steady swelling. Based on these results, at least part of the incubation behavior may be identified with the development of large, stable voids, supporting the use of nucleation and growth simulations [12–14] for transient swelling behavior.

While such calculations give a plausible incubation [11, 15], they fail to reproduce many qualitative features of experimental swelling. For example, much of the acceleration of swelling during the experimental incubation period occupies only a fraction of its duration, towards the end of the interval. In general, those experiments with the longest incubation delays exhibit the sharpest crossover to steady swelling [1]. In contrast, the predicted swelling is found to rise smoothly during incubation. The longest delays are the most gradual, swelling with a power-law behavior versus time [15]. Additionally, while the experimental swelling appears to be steady after incubation [1], the predicted swelling rate declines with time. The calculated peak rate can fall by half at 100 dpa [15]. Finally, the experimental

steady swelling rates are largely independent of temperature and flux over wide ranges [1]. In contrast, the simulated swelling is visibly dependent on the temperature and dose rate. The predicted swelling curves at different temperatures tend to cross one another because the longer incubation cases seem to lead to higher peak swelling rates [15]. The predicted incubation delay is very short, roughly consistent with experiments on high-purity steel, but the different flux-dependence suggests that another process in the overall microstructural evolution (besides void nucleation and growth) explains the observations there.

It is well known that dislocation densities simultaneously evolve with the voids under irradiation bombardment. The resulting time-dependent changes in the dislocation sink strength will influence the predicted swelling behavior. Thus, co-evolution of dislocations should be included along with the careful modeling of voids when comparing rate-theory simulations to observations. Realistic simulations of co-evolving dislocation and void populations have recently been performed, and a preliminary examination of a combined dislocation/void evolution model shows encouraging results for swelling behavior [16]. In this paper, we report on further simulations of void and dislocation co-evolution. We model an impurity-free, type-316 stainless steel, with a starting dislocation density of 6×10^{13} m^{-2}, corresponding to a solution annealed starting material. We examine incubation times, quasi-steady swelling rates, and terminal void and dislocation densities and their dependence on temperature, flux, and dose.

These simulations reveal how the dislocation and void sinks depend self-consistently on the mobile defect population and thus on environmental parameters like temperature and flux. The final density of (stable, visible) voids depends on the initial dislocation density, besides environmental parameters. The terminal dislocation density is mainly a function of temperature and flux and the final void density; it is not directly dependent on the original dislocation content. Unstable clusters never reach an asymptotic concentration; they are sustained by the evolving vacancy supersaturation (itself a function of the environment and the evolving void and dislocation content). The competition among these three temperature-, flux-, and time-dependent sinks creates a nearly constant swelling rate in %/dpa for a wide range of environments. To understand this result, the flow of radiation-induced defects is crudely analyzed by comparing total sink strengths of the dislocations and voids. Based on this analysis, the improved agreement with experiment may be attributed to a reduced

nucleation of voids in the solution-annealed material, followed by the increase of dislocation density and dislocation sink strength (by approximately an order of magnitude).

II. TIME-DEPENDENT DISLOCATION MODEL

During irradiation, dislocation evolution depends on thermal annealing processes, a net influx of radiation-induced defects to pre-existing dislocations, and loop nucleation directly from the non-equilibrium vacancy and interstitial populations under irradiation. The overall behavior has been examined in an earlier study, assuming that dislocation segments experience a range of different local environments [17]. With one free parameter, the model obtains reasonable results for dislocation content versus temperature, time, and irradiation flux as compared to experiment. The result is expressed with separate annihilation and production processes:

$$\frac{d\rho}{dt} = -A\rho^2 + B\rho \tag{1}$$

in terms of the dislocation density, ρ.

The quadratic term is consistent with dislocation dipole annihilation. Its prefactor is obtained from a detailed model for the rate of dipole annihilation under combined glide and climb of dislocation segments. Segment motion is driven both by thermal annealing and by the non-equilibrium flux of mobile defects due to irradiation. Individual dislocation segments receive a net flux of vacancies or interstitials (even in the absence of voids) because the local environments and bias factors of the dislocation segments are assumed to vary by random amounts. The separate term for production of dislocation segments, $B\rho$, models the process as dislocation bowing between pinning points under the net supersaturation of defects. The linear dependence is consistent with production at Frank-Read sources. The prefactor depends on an average separation of pinning points, l (which is the only adjustable parameter). The pinning density is fit to the measured terminal dislocation density at some temperature and dose rate. Ultimately, segment annihilation (creation) is not strictly quadratic (linear) in the density, since the coefficients, A and B, are also functionally dependent on ρ.

This dislocation evolution model has been incorporated into simulations for void nucleation and growth [16]. The time-dependent defect flux to dislocations is proportional to

the instantaneous monomer concentrations, and so depends indirectly on the sink strength for the co-evolving voids, as well. Vacancy and interstitial concentrations are calculated in a quasi-static approximation, assuming that all irradiation damage is introduced as defect monomers and including the sink strength of the voids and dislocations in mean field. Dislocations are modeled as consisting exclusively of network dislocations. (The bias factors assume straight dislocation segments in a uniform environment, independent of the instantaneous dislocation density. As a result, void populations and dislocation density co-evolve in a partial self-consistency with the instantaneous supersaturation of vacancies and interstitials. That is, the dislocation evolution model assumes that there are variations in local environment and that dislocation segments can bow, but the monomer rate theory calculation does not.)

The computational method for treating void evolution has also been previously described in detail [11]. Vacancy clusters are considered to be spherical particles, and the cross-section for monomer impingement taken to be proportional to the sum of cluster and vacancy radii. Stress-induced interactions and bias factors are calculated in an approximate mean field treatment. Thermal vacancy emission rates are obtained from a fit to cluster energies and a time-reversal argument. Cluster growth and evaporation are treated stochastically, to capture the nucleation of stable clusters including transient behavior. The entire, coupled system of monomers, dislocations, and voids can be evolved numerically to cumulative doses in excess of 100 dpa.

III. RESULTS AND ANALYSIS

The initial swelling behavior for void and dislocation co-evolution in type-316 stainless steel is shown in Fig.1. Model parameters are the same as were used for earlier, constant dislocation density simulations. (Representative swelling curves for that model may be seen in Ref. [11].) In the simulations reported here, the swelling curves at multiple temperatures appear to reach the same asymptotic swelling rate, around 0.8 %/dpa. The exact value depends on the bias factor model chosen for the dislocations [18]. The highest temperature case shown (660 C) is still in the incubation stage at 25 dpa; it increases to a swelling rate of approximately 0.5 %/dpa by the end of the simulation at 100 dpa. Incubation periods are

visibly much shorter than are seen in commercial reactor steels. However, experiments on high-purity ternary stainless steels have a much shorter incubation delay than commercial steels [3–7]. Such pure materials are closer to our model for precipitate- and solute-free steel. Our two principal results, namely, the incubation-like interval followed by steady swelling that is uniform over a range of temperatures, are in good qualitative agreement with experiment.

The predicted crossover from transient to steady swelling is slightly more abrupt now that dislocation evolution is included. However, the behavior still does not precisely mimic the available experimental data for commercial steels. This predicted crossover may be a characteristic of high-purity material, or an artifact of the approximations made. As yet, there are few detailed measurements of the crossover in such high-purity systems.

The simulations may be numerically differentiated to obtain the swelling rate versus time or dose. This is shown in Fig. 2, for the full duration of the simulation. There are three changes between the current results and those with a time-independent dislocation model (Ref. [11, 15]). First, the swelling takes longer to reach its peak rate. Second, the swelling rate does not always show a single local maximum, which it invariably does when the dislocation content is held fixed. Finally, the peak swelling rates are better maintained at late times. (For example, the swelling rate at 500 C remains between 0.7 and 0.9 %/dpa from 1 to 100 dpa.)

These differences are all consequences of the evolving dislocation density, which increases from its solution-annealed starting values to a temperature- and flux-dependent terminal value. In a fixed dislocation density model, the voids monotonically grow to become the dominant sinks for vacancies and interstitials. The net swelling rate is initially small when there are few voids present, then increases (incubation behavior) to a maximum value as the stable voids nucleate and grow, and finally declines (quasi-steady behavior) as the void sink strength increases to dominate the dislocations. As this occurs, interstitials increasingly annihilate at the stable voids instead of contributing to dislocation climb, causing the swelling rate to diminish [19]. In contrast, when the dislocation density is allowed to evolve from starting solution-annealed values, the dislocation sink strength also increases monotonically from initial values. The relative strength of voids versus dislocations changes more slowly. As a result, the swelling rate can have more than one local extremum, and the peak rate

of swelling appears to be better maintained over time. Ultimately, the dislocation density reaches saturation while the voids continue to grow in size. The swelling behavior then resembles the model with a constant dislocation density.

The co-evolution model predicts relatively simple behavior for dislocation and void densities (Figs. 3 and 4). For most (moderate) temperatures, the dislocation density increases from the starting value of 6×10^{13} m^{-2}. Time-evolution is faster for higher temperatures and dislocation mobility. The terminal dislocation density declines with temperature (for a fixed irradiation rate) as dipole annihilation increases in importance [17]. Visible voids (Fig. 4) nucleate rapidly and reach their approximate terminal densities in fractions of a dpa. Comparing Figs. 3 and 4 demonstrates that void nucleation is completed before the dislocation density changes appreciably. Terminal (stable) void density thus depends on temperature, dose rate, and starting dislocation density, but is independent of terminal dislocation density.

The ratio of the evolving void sink strength to the dislocation sink strength is shown in Fig. 5. A unit ratio is commonly considered to achieve steady swelling, by providing for the most efficient segregation of vacancies and interstitials. The simulations demonstrate that the relative sink strength is essentially never close to unity. Instead, the ratio transiently reaches large values due to the formation of numerous small, unstable clusters [20]. By the time the vacancy concentration falls and the unstable clusters are reduced in density, the stable voids have grown to provide the dominant sink strength.

Ultimately, the predicted steady-swelling rate lies near 1%/dpa because the underlying defect production rate (0.1 Frenkel pair per dpa) and stress-induced bias factors reproduce the experimentally observed rate of vacancy/interstitial segregation for the high ratio of sink strengths. The swelling is quasi-steady because the defect sinks stay in a narrow post-incubation range (near 2:1 to 4:1) for the length of the simulation and for a wide range of temperature. Two factors help preserve this ratio. First, for most temperatures, fewer stable voids nucleate when the initial dislocation content is low (see Fig. 12, Ref. [15]). Thus, for a given amount of swelling, solution-annealed initial conditions give fewer, larger stable voids. This better preserves the ratio of sink strengths over subsequent volume changes [21]. Second, the solution-annealed dislocation density increases to a terminal value (typically by a factor of 10) after the stable voids have nucleated. This makes the ratio of sink strengths

even less sensitive to the chronic void growth and thereby prolongs the quasi-steady swelling behavior [22].

Besides the steady-swelling behavior, we obtain encouraging results on the temperature- and flux-dependent trends in the incubation delay. Fig. 6 shows the predicted incubation time for high-purity type-316 stainless steel as a function of temperature and for three different dose rates. The incubation curves qualitatively resemble simulations where the dislocation density is constrained at the approximate terminal density (6×10^{14} m^{-2}, see Fig. 6, Ref. [15]), although the curves seem to shift to slightly higher temperature here. As before [15], the family of curves in Fig. 6 shows that the location of the peak swelling temperature (shortest incubation) shifts to higher temperatures as the flux increases. They also show a so-called dose-rate effect. For moderate temperatures (less than 500-600 C), the lower flux cases have the shorter incubation doses. At higher temperatures, the flux effect mainly acts to shift the upper temperature boundary above which swelling is greatly suppressed.

Figure 7 displays another definition of the incubation time, namely a linear extrapolation from the steady-swelling portion of the curve back to the abscissa (called the tangent construction here). This definition of incubation gives a stronger dose-rate effect near 400 C. Experimental measurements on high purity ternary steel between 408 and 440 C give a dose-rate effect of the same sign, namely, that the lower flux has the smaller incubation dose [4, 5]. However, the experimental result is much stronger than predicted. Fluxes around 10^{-8} dpa/s possess incubation times of less than 1 dpa, while 10^{-6} dpa/s shows incubation delays of some 30 dpa. Experiments in commercial steel show a much weaker flux effect (i.e., more consistent with the magnitude of the simulated effect), with longer incubation times [1].

Finally, the terminal void density is shown in Fig. 8. This refers to clusters that should be "visible" to TEM, namely, those with radius $r > 0.5$ nm, for comparison with experimental measurements. The results differ from those shown in Fig. 7, Ref. [14], because of changes in both the numerical treatment and in the dislocation bias factors. The new results are in good agreement with experiment.

IV. CONCLUSIONS

The predicted swelling behavior changes significantly when dislocation co-evolution is included along with void nucleation and growth. The crossover from incubation behavior to steady growth is more abrupt than when the dislocations are held constant. The simulations still do not precisely mimic the behavior seen in commercial reactor steels. However, the model is appropriate to high-purity rather than commercial alloys. The predicted temperature- and flux-dependent incubation time is qualitatively consistent with observations for high purity ternary steel. However, the available measurements suggest a stronger flux-dependence, resembling an inverse relation between incubation dose and dose-rate.

Once incubation is complete, the simulated quasi-steady swelling rate is now more nearly constant versus time and shows a greatly reduced dependence on temperature and dose rate. The evolution in dislocation density from the solution-annealed starting point towards the terminal value is required to predict this realistic swelling behavior. At most temperatures studied, the dislocation density increases from its solution-annealed starting values, along with the growing void sinks. This prolongs the period of steady swelling as compared to calculations with a fixed dislocation content.

On the other hand, the predicted terminal void density is similar whether a fixed or time-dependent dislocation density is used. This is because the stable voids nucleate very quickly in the simulation, before the dislocation density can change appreciably from its initial values. The predicted stable void density is also in good agreement with experiment.

These dislocation and void co-evolution calculations use time-independent (i.e., independent of the evolving dislocation density) dislocation bias factors. This is an approximation, since the factors will depend on the details of the dislocation environment, including separation from nearby dislocation segments. The constant bias factors appear to give good results for the terminal void densities. However, they underestimate the incubation times, even for experiments in high-purity steel. The further, separate modeling of network and loop dislocation will allow refinements to the model like more accurate, time-dependent dislocation

bias factors. An improved dislocation evolution model is planned for future work.

---

[1] F. Garner, in *Nuclear Materials* (1994), vol. 10A, chap. 6, p. 419.

[2] F. A. Garner, M. B. Toloczko, and B. H. Sencer, Journal of Nuclear Materials **276**, 123 (2000).

[3] T. Okita, T. Kamada, and N. Sekimura, Journal of Nuclear Materials **283–287**, 220 (2000).

[4] T. Okita, Ph.D. thesis, Tokyo (2000).

[5] T. Okita, T. Sato, N. Sekimura, and F. A. Garner, in *Proceedings of the Fourth Pacific Rim International Conference on Advanced Materials and Processing* (Aoba,Aramaki,Aoba-ku,Sendai, 2001), vol. PRICM-4.

[6] T. Okita, T. Sato, N. Sekimura, F. A. Garner, L. R. Greenwood, and W. G. Wolfer, in *Proceedings of the 10th International Symposium on Environmental Degradation of Materials in Nuclear Power Systems - Water Reactors* (2001).

[7] T. Okita, T. Sato, N. Sekimura, F. A. Garner, and L. R. Greenwood, Journal of Nuclear Materials **307–311**, 322 (2002).

[8] A. D. Brailsford and R. Bullough, Journal of Nuclear Materials **44**, 121 (1972).

[9] J. Katz and H. Wiedersich, Journal of Chemical Physics **55**, 1414 (1971).

[10] K. Russell, Acta Metallurgica **26**, 1615 (1978).

[11] M. P. Surh, J. B. Sturgeon, and W. G. Wolfer, Journal of Nuclear Materials **325**, 44 (2004).

[12] W. G. Wolfer and A. Si-Ahmed, Philosophical Magazine A **46**, 723 (1982).

[13] B. B. Glasgow, A. Si-Ahmed, W. G. Wolfer, and F. A. Garner, Journal of Nuclear Materials **103**, 981 (1981).

[14] M. F. Wehner and W. G. Wolfer, Philosophical Magazine A **52**, 189 (1985).

[15] M. Surh, J. Sturgeon, and W. Wolfer, to be published (2004).

[16] M. P. Surh, J. B. Sturgeon, and W. G. Wolfer, in *Effects of Radiation on Materials: 21st International Symposium, ASTM STP 1447*, edited by M. L. Grossbeck, T. R. Allen, R. G. Lott, and A. S. Kumar (ASTM International, West Conshohocken, PA, 2003), vol. ASTM STP 1447.

[17] W. G. Wolfer and B. B. Glasgow, Acta Metallurgica **33**, 1997 (1985).

[18] (We use constant (density-independent, but temperature-dependent) bias factors calculated

for a density of 6×10^{14} m^{-2}.).

[19] L. Mansur, Journal of Nuclear Materials **206**, 306 (1993).

[20] (Here, "unstable clusters" includes the vacancy monomers as well as small voids. Thus, the unstable cluster sink strength gives a measure of the vacancy-interstitial recombination plus vacancy-interstitial recombination at vacancy clusters.).

[21] (Once stable voids have finished nucleating, the steady swelling increases their average volume in proportion to the macroscopic volume change. However, sink strengths increase as the void radius, so the total change in sink strength versus volume change is less when there are fewer voids in the system.).

[22] (For example, the declines from the peak in the log-linear plots from Fig. 2 (e.g., for 340 to 580 C) have approximately the same slope as in Ref. 15 achieved much later (near 10 dpa instead of 1 dpa), so the drop at 100 dpa is much smaller.).

FIG. 1: Volumetric swelling versus dose to 100 dpa for multiple temperatures and for a dose rate of 10^{-6} dpa/s. The temperatures are listed in the figure legend.

FIG. 2: Swelling rate versus dose for the same temperatures and dose rates as Fig. 1. The roughly straight, declining segments that follow the peaks (e.g., for the curves at 340 to 580 C between 20 and 100 dpa) are a characteristic of void sinks that eventually grow to dominate the asymptotic dislocation sinks (see also Fig. 3, Ref. [15]

FIG. 3: Dislocation density versus dose for various temperatures and a dose rate of 10^{-6} dpa/s.

FIG. 4: Visible void density versus dose for various temperatures and a dose rate of 10^{-6} dpa/s. This quantity is a reasonable surrogate for the density of stable voids (i.e., those that continue to grow under the supersaturation of vacancies).

FIG. 5: Ratio of the unbiased sink strengths of voids to dislocations as a function of dose. The void sink strength includes unstable vacancy clusters and vacancy monomers as well as all of the stable voids.

FIG. 6: Incubation dose versus temperature for three irradiation dose rates, of 10^{-6} , 10^{-7}, and 10^{-8} dpa/s. The incubation is defined using a threshold swelling of 1%.

FIG. 7: Incubation dose versus temperature for three irradiation dose rates, of 10^{-6} , 10^{-7}, and 10^{-8} dpa/s. The incubation is defined using a tangent construction from the point of maximum slope in the swelling curves.

FIG. 8: Terminal density of visible voids (taken at 100 dpa total fluence) versus temperature for three irradiation dose rates, of 10^{-6} , 10^{-7}, and 10^{-8} dpa/s.

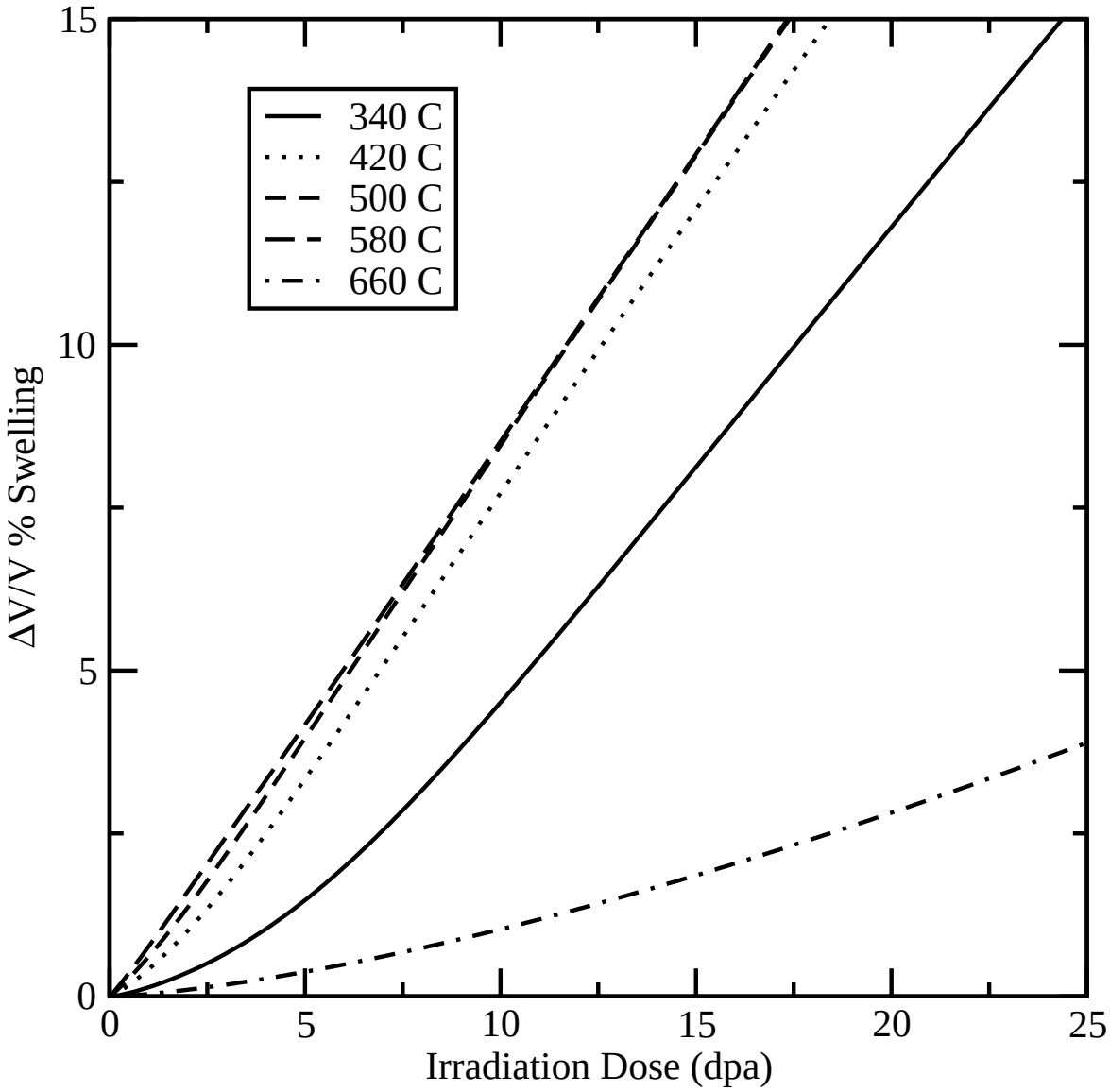
15
10
5
0
0
5
10
15
20
25
ΔV/V % Swelling
Irradiation Dose (dpa)
340 C
420 C
500 C
580 C
660 C

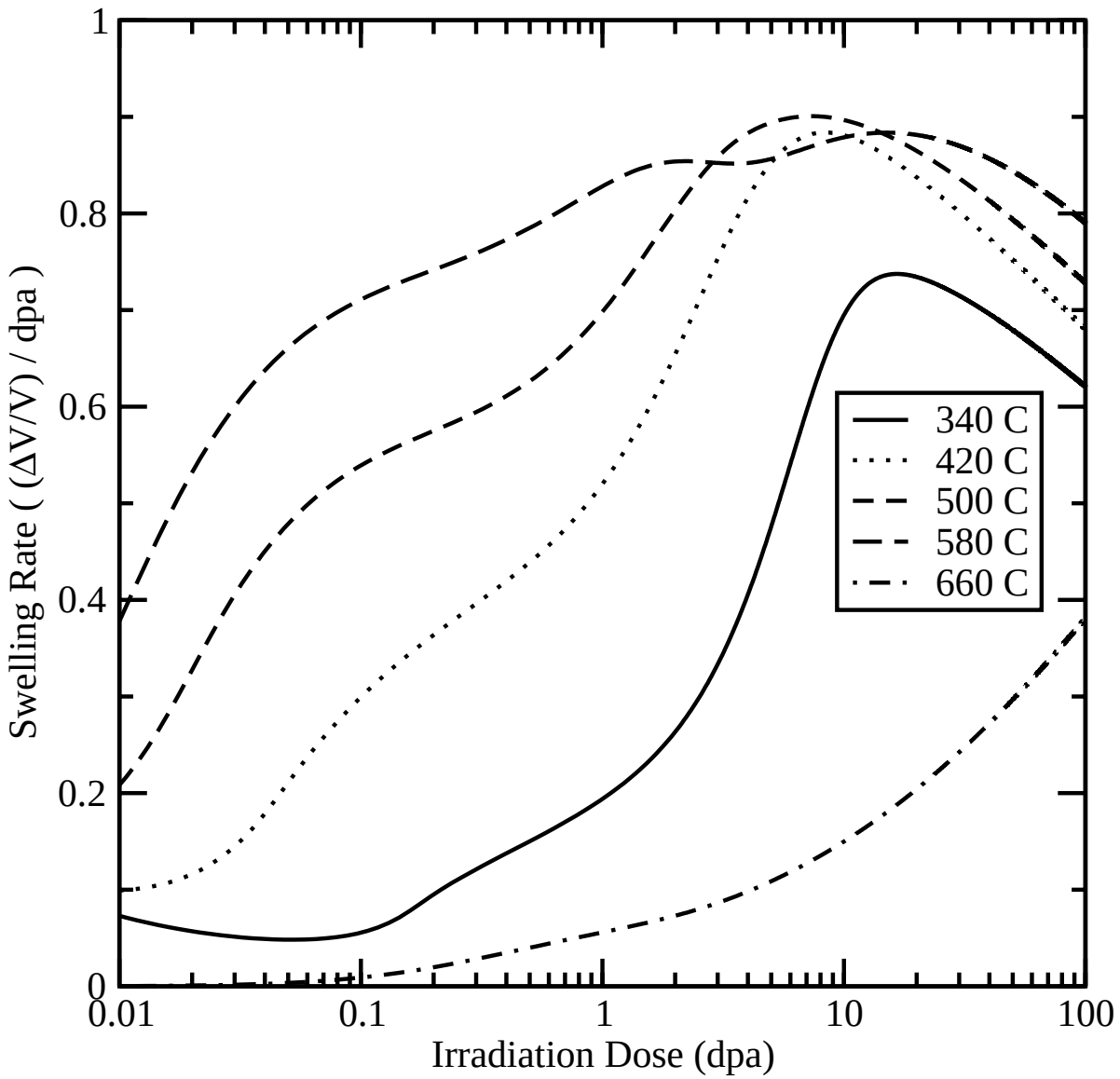
1
0.8
0.6
0.4
0.2
0
0.01
0.1
1
10
100
Swelling Rate ((ΔV/V) / dpa)
Irradiation Dose (dpa)
340 C
420 C
500 C
580 C
660 C

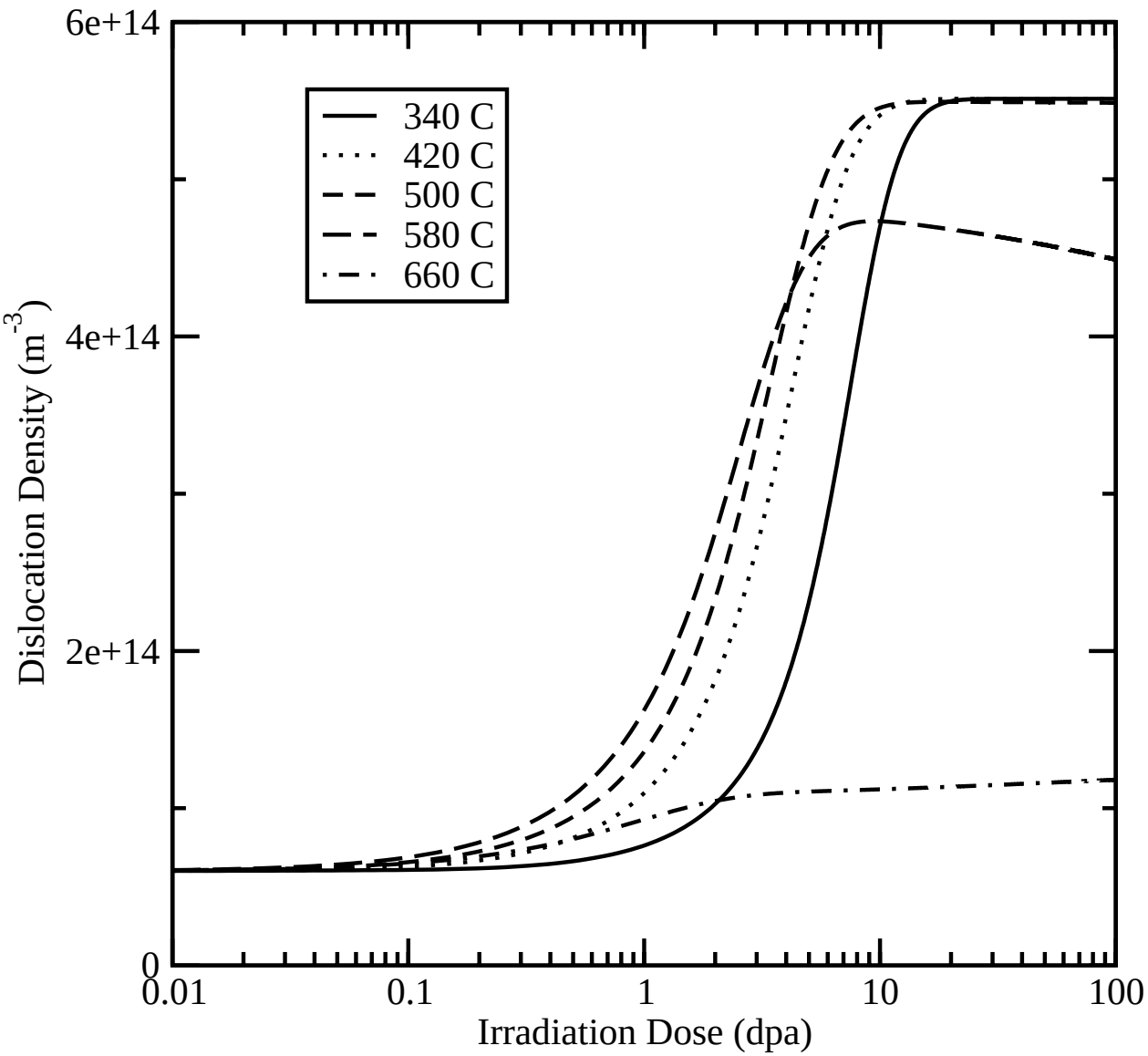
6e+14
4e+14
2e+14
0
0.01
0.1
1
10
100
Dislocation Density (m-3)
Irradiation Dose (dpa)
340 C
420 C
500 C
580 C
660 C

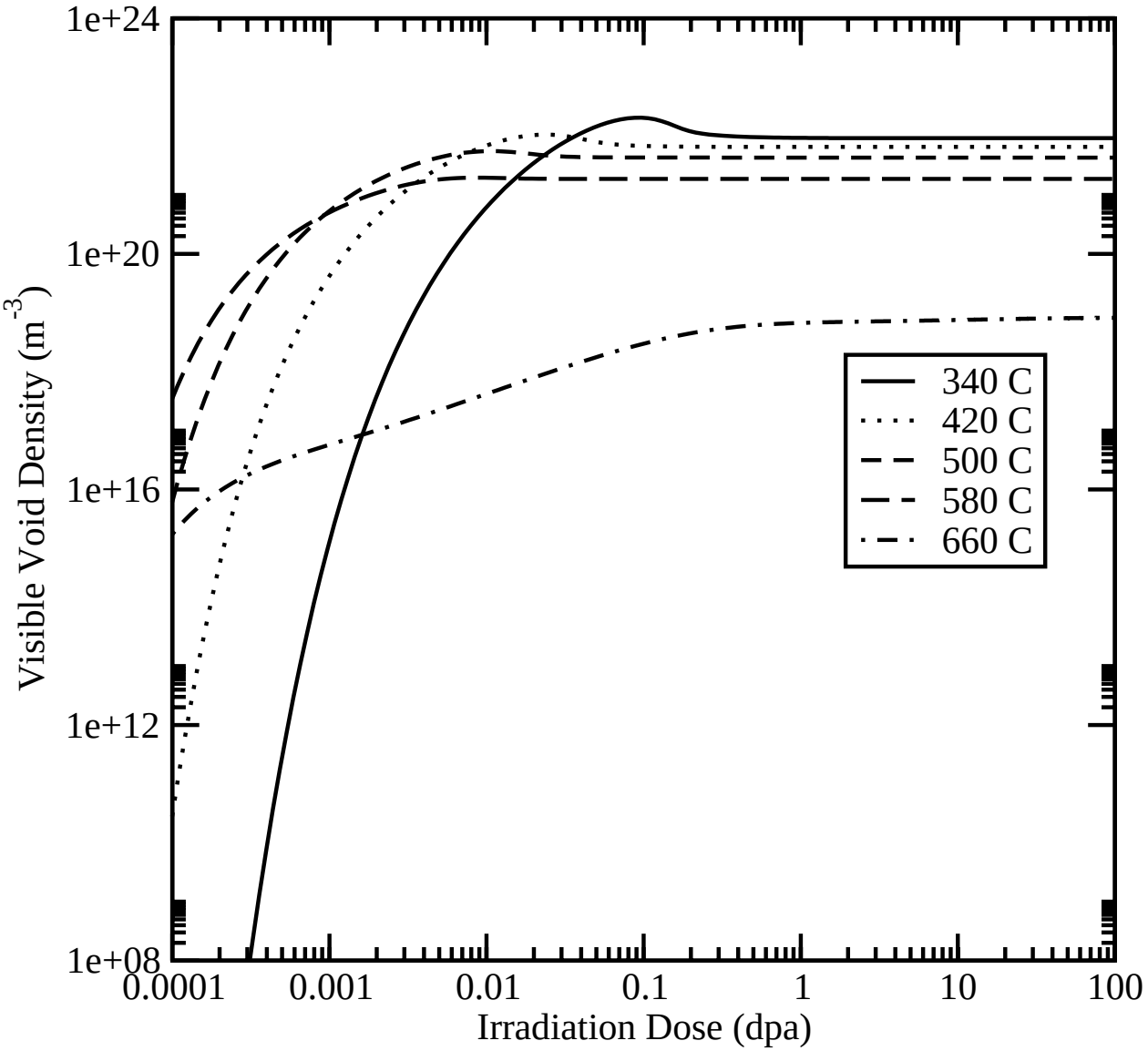
1e+24
1e+20
1e+16
1e+12
1e+08
Visible Void Density (m-3)
0.0001
0.001
0.01
0.1
1
10
100
Irradiation Dose (dpa)
340 C
420 C
500 C
580 C
660 C

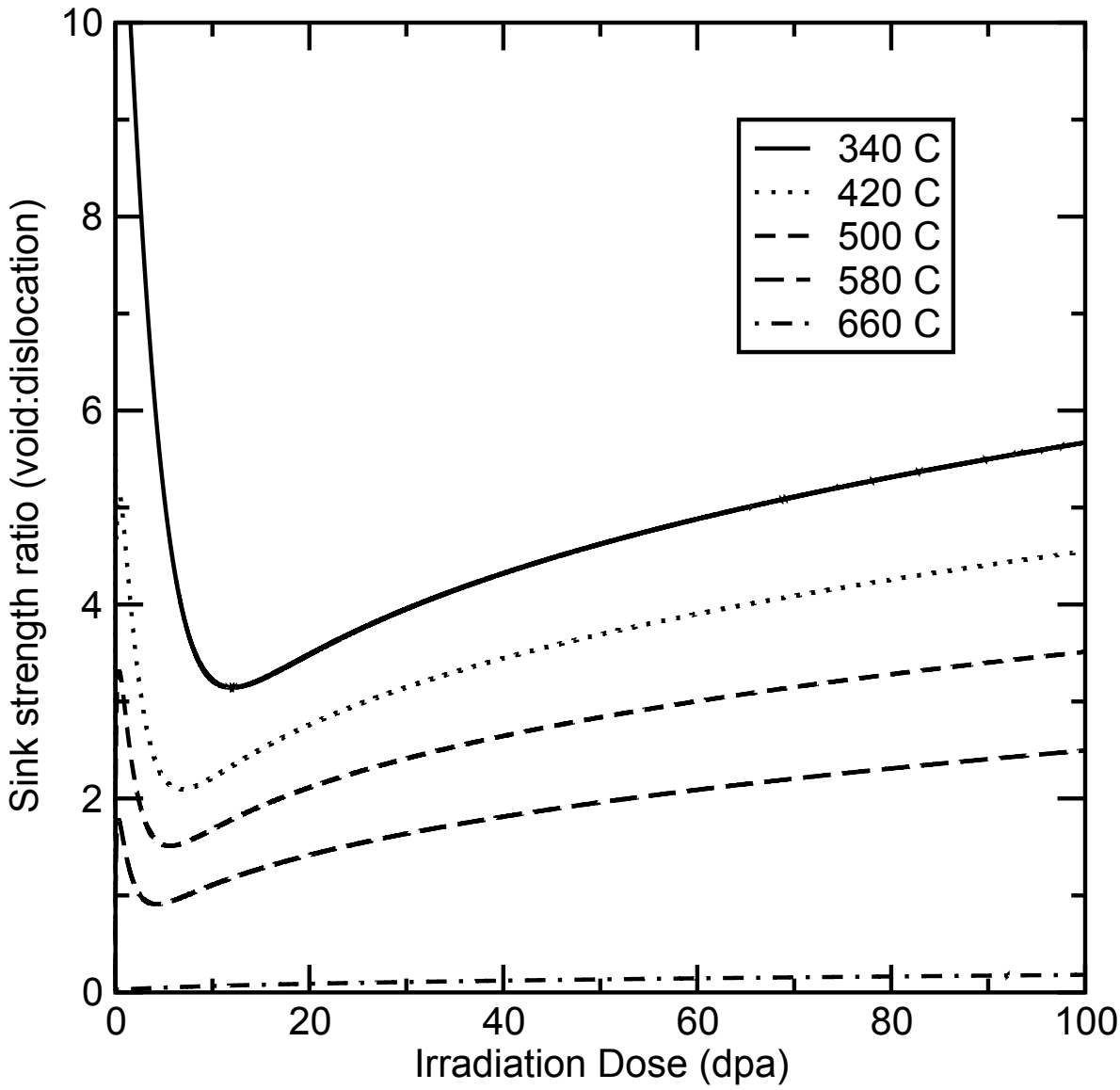
10
8
6
4
2
0
0
20
40
60
80
100
Sink strength ratio (void:dislocation)
Irradiation Dose (dpa)
340 C
420 C
500 C
580 C
660 C

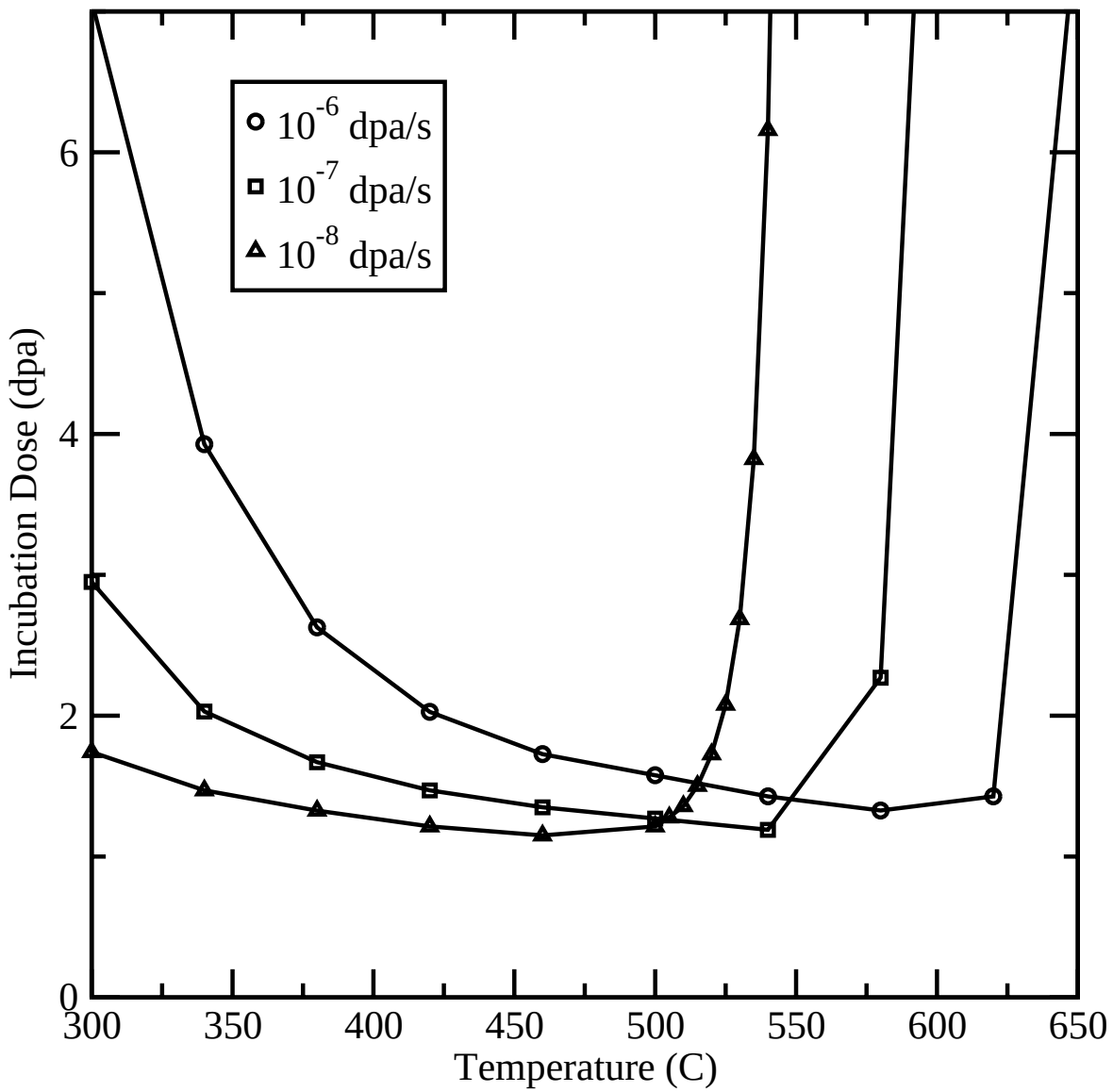
10^-6 dpa/s
10^-7 dpa/s
10^-8 dpa/s
Incubation Dose (dpa)
Temperature (C)
0
2
4
6
300
350
400
450
500
550
600
650

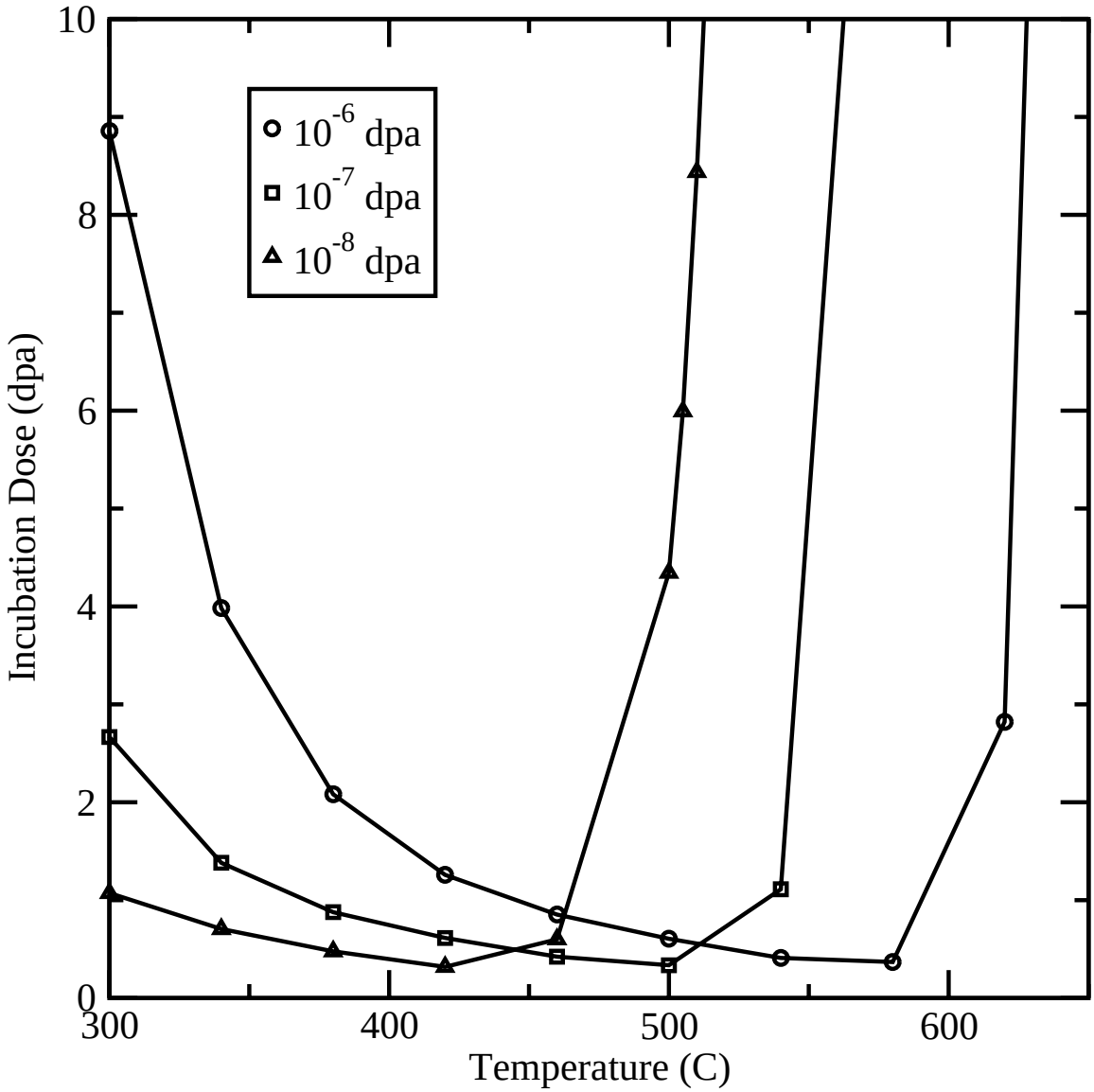
10
8
6
4
2
0
300
400
500
600
Incubation Dose (dpa)
Temperature (C)
10^-6 dpa
10^-7 dpa
10^-8 dpa

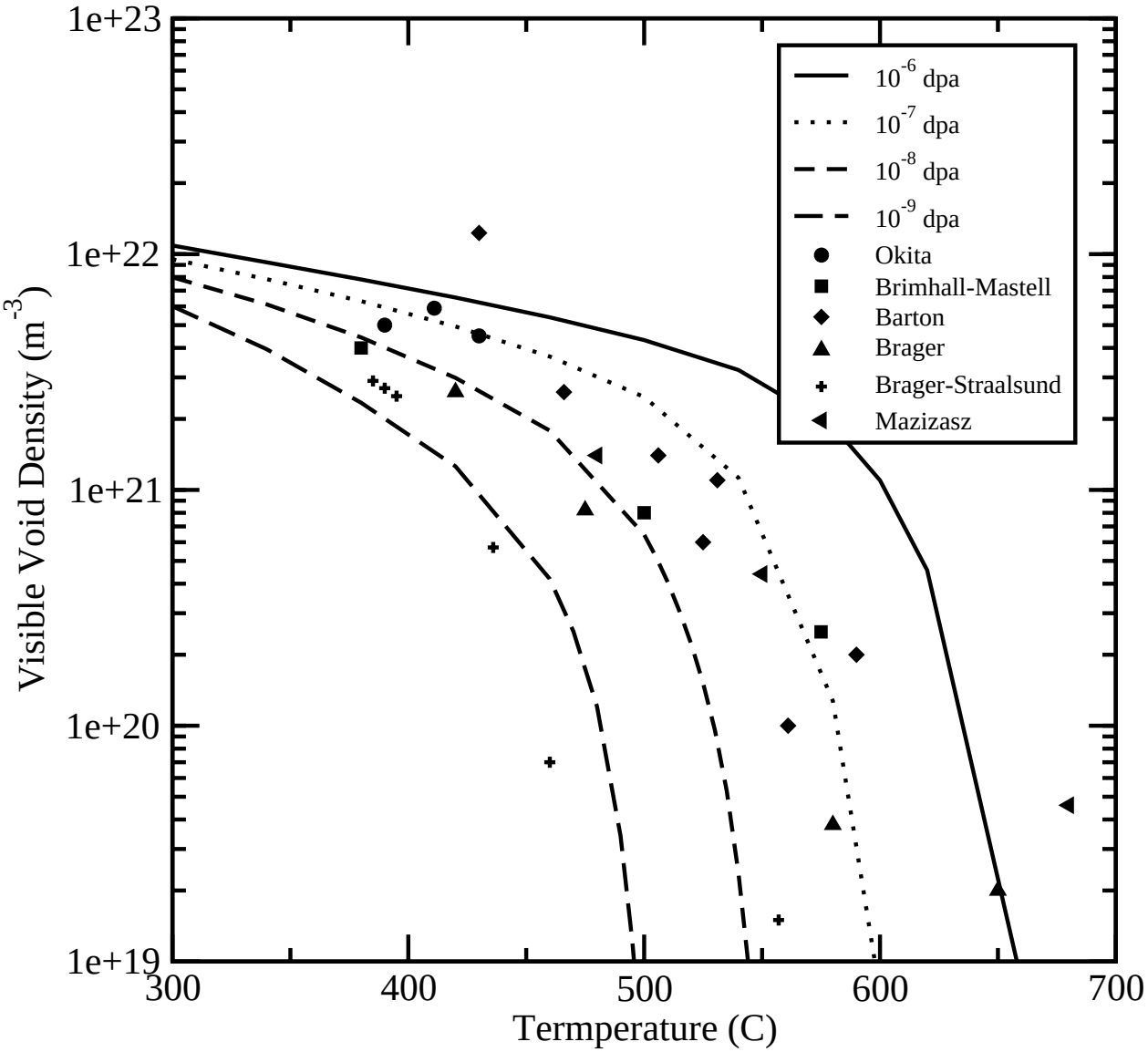
1e+23
1e+22
1e+21
1e+20
1e+19
300
400
500
600
700
Visible Void Density (m-3)
Termperature (C)
10-6 dpa
10-7 dpa
10-8 dpa
10-9 dpa
Okita
Brimhall-Mastell
Barton
Brager
Brager-Straalsund
Mazizasz